



## Regional aboveground live carbon losses due to drought-induced tree dieback in piñon–juniper ecosystems

Cho-ying Huang<sup>a,b,\*</sup>, Gregory P. Asner<sup>a</sup>, Nichole N. Barger<sup>c</sup>, Jason C. Neff<sup>d</sup>, M. Lisa Floyd<sup>e</sup>

<sup>a</sup> Department of Global Ecology, Carnegie Institution for Science, Stanford, CA 94305, USA

<sup>b</sup> Department of Geography, National Taiwan University, Taipei 10617, Taiwan

<sup>c</sup> Department of Ecology and Evolutionary Biology, University of Colorado, Boulder, CO 80309, USA

<sup>d</sup> Geological Sciences and Environmental Studies Departments, University of Colorado, Boulder, CO 80309, USA

<sup>e</sup> Environmental Studies Program, Prescott College, Prescott, AZ 86301, USA

### ARTICLE INFO

#### Article history:

Received 18 February 2009

Received in revised form 26 October 2009

Accepted 6 February 2010

#### Keywords:

Bark beetle

Carbon storage

Colorado Plateau

*Juniperus osteosperma*

Landsat

*Pinus edulis*

Spectral mixture analysis

Tree mortality

Wildfire

### ABSTRACT

Recent large-scale dieback of piñon–juniper (P–J) woodlands and forests across the western US occurred as a result of multi-year drought and subsequent insect and disease outbreaks. P–J vegetation is spatially extensive, thus large-scale mortality events such as the one that has occurred over the past several years could significantly alter regional carbon (C) budgets. Our objective was to use a remote sensing technique coupled with field-based data to estimate changes in aboveground live C stocks across a 4100 km<sup>2</sup> region of Colorado caused by P–J tree mortality. We hypothesized that dieback would amplify the phenological dynamics of P–J vegetation, and these variations would be related to drought-induced losses of live P–J aboveground biomass (AGB) that are discernible using time-series remote sensing vegetation data. Here, we assess live P–J AGB loss using dry season fractional photosynthetic vegetation cover (PV) derived from multi-year Landsat images. Our results showed a strong linear positive relationship between the maximum decline in PV and field-measured losses of live P–J AGB during the period 2000–05 ( $r^2 = 0.64$ ,  $p = 0.002$ ). These results were then used to map AGB losses throughout the study region. Mean live aboveground C loss ( $\pm$  sd) was 10.0 ( $\pm 3.4$ ) Mg C ha<sup>-1</sup>. Total aboveground live P–J C loss was 4.6 Tg C, which was approximately 39 times higher than the concurrent C loss attributed to wildfire and management treatments within or near to the national forests of the study region. Our results suggest that spatially extensive mortality events such as the one observed in P–J woodlands across the western US in the past decade may significantly alter the ecosystem C balance for decades to come. Remote sensing techniques to monitor changes in aboveground C stocks, such as the one developed in our study, may support regional and global C monitoring in the future.

© 2010 Elsevier Inc. All rights reserved.

### 1. Introduction

Carbon (C) dynamics during and following major disturbance events in forest and woodland ecosystems have been recognized as potentially important but poorly understood components of C budgets of North America (van Mantgem et al., 2009). Over the past several years drought-induced mortality, and subsequent insect and disease outbreaks, have been observed across a range of forest types in western North America (Pennisi, 2009). Tree mortality has climbed upwards by 90% in some forest stands and tree loss at this intensity and spatial scale has the potential to significantly alter regional C storage in western forest and woodland types for decades into the future (Breshears et al., 2005; Kurz et al., 2008; Shaw et al., 2005). Thus developing techniques to monitor landscape level changes in C storage associated with large-scale mortality events is critical, not only to our understanding of short-

and long-term C dynamics in these ecosystems, but also to a better managing for biospheric C storage.

Piñon (*Pinus edulis*, *P. monophylla*) and juniper (*Juniperus osteosperma*, *J. monosperma*) (P–J) woodlands are widespread vegetation types occupying approximately 18% (220,000 km<sup>2</sup>) of the natural vegetation in the southwestern US landscapes (Lowry et al., 2007). The recent multi-year drought across the Southwest began in 1998, but the intensity of the drought has been variable throughout the region (McPhee et al., 2004). Anecdotal reports of drought affecting P–J woodlands started in 2000, and massive tree dieback, which took place predominantly across piñon pine populations with junipers remaining relatively unimpacted, occurred in 2002 (Shaw et al., 2005). According to yearly large-scale (83,000 km<sup>2</sup>) aircraft-based field surveys (Drought Impact on Regional Ecosystems Network; <http://mprlsvr1.bio.nau.edu/direnet/>), approximately 11% of the P–J vegetation in the Colorado Plateau was infested by insects during 2000–05. However, spatial patterns of tree mortality are patchy (Kurz et al., 2008), and are influenced by factors such as stand density, age and topography (Greenwood & Weisberg, 2008). Other studies show that the green

\* Corresponding author. Tel.: +886 2 3366 3733; fax: +886 2 2362 2911.

E-mail address: [choying@ntu.edu.tw](mailto:choying@ntu.edu.tw) (C. Huang).

vegetation cover might decline due to the acceleration of runoff and soil erosion after dieback induced surface fire (post-fire scenario, Fig. 1) (Allen, 2007), or space left by dead P–J may be occupied by herbaceous plants following a major rainfall event (herbaceous ramp-up scenario, Fig. 1) (Rich et al., 2008).

Although it is possible to derive woody aboveground biomass (AGB) across large forested regions using remote sensing techniques (Goetz et al., 2009; Zheng et al., 2004), it is generally more difficult to do so in arid and semi-arid environments due to the complexity of land surfaces (Goslee et al., 2003; Scanlon et al., 2002; Weisberg et al., 2007). One effective strategy is to derive woody photosynthetic vegetation cover (PV) from fine spatial resolution, multi-spectral satellite images collected in the dry season using spectral mixture analysis (Adams et al., 1993; Bradley & Fleishman, 2008). Estimates of PV can then be converted to AGB based upon field-estimated allometric relationships because the crown cover tends to scale with stand-level biomass stocks in these open woodland systems (Asner et al., 2003; Huang et al., 2007). PV in drylands is dominated by woody vegetation when the remote sensing data are acquired during the dry season, a time when the majority of herbaceous plants (grasses, sedges and forbs) are senescent. Therefore, a rapid reduction of remotely sensed tree cover through the drought years (time-series) could indicate the loss of live tree AGB (defined as converting live trees to dead woody materials such as coarse woody debris, red- and gray colored needles, etc.) regardless of the post dieback conditions (Fig. 1). Following this approach, a large-scale assessment of the impacts of tree dieback on C storage might then be performed. In this study, we addressed the following questions: (a) what are the impacts of tree dieback on the regional live C stocks in P–J ecosystems? and (b) what is the feasibility and potential for utilizing time-series multi-spectral satellite data to estimate changes in live C stocks in P–J systems?

## 2. Methods

### 2.1. Site description

This study was conducted in P–J ecosystems of southwestern Colorado encompassed by a set of Landsat Worldwide Reference System (WRS-P35R34) (The Landsat Program; <http://landsat.gsfc.nasa.gov/about/wrs.html>). The spatial extent of the study region is approximately 4100 km<sup>2</sup> determined from the southwest Regional

Gap Analysis Program (ReGAP) vegetation coverage (Lowry et al., 2007) (Fig. 2), and covers two national forests (Uncompaghre and San Juan) and nine counties (Archuleta, Dolores, Gunnison, Hinsdale, La Plata, Montezuma, Montrose, Ouray and San Miguel). The elevation range of the P–J vegetation in the study area is about 1400–2800 m. The climate of the region is generally temperate and semi-arid. Mean ( $\pm$  standard deviation, sd) annual precipitation and temperature of the study region are 389 ( $\pm$ 60) mm and 8.5 ( $\pm$ 1.1) °C, respectively, according to long-term interpolated climate records (1895–2006) from the PRISM (Parameter-elevation Regressions on Independent Slopes Model) (Daly et al., 1994). Dominant overstory trees across the study area are Colorado piñon (*P. edulis*) and Utah juniper (*J. osteosperma*), understory shrubs including serviceberry (*Amelanchier utahensis*), antelope bitterbrush (*Purshia tridentata*), Gambel oak (*Quercus gambelii*) and sagebrush (*Artemisia* spp.), and cold season perennial bunchgrasses.

US Forest Service Forest Inventory Analysis (FIA) annual inventory indicated that the P–J vegetation of the study region suffered the most severe tree dieback during the recent drought period in the southwestern US. In some areas, up to 100% of piñon pines were killed (Shaw et al., 2005). The drought across our study region, defined as rainfall failing to reach the long-term average over consecutive months and years resulting in declines in water supply, began in 2000 and lasted for four consecutive years (2000 = –25 mm mean annual precipitation, 2001 = –59 mm; 2002 = –126 mm, 2003 = –49 mm) (Fig. 3b). Throughout this period the mean annual air temperature was about 1.1 °C above the long-term average with the occurrence of several consecutive dry/hot months (Fig. 3b). FIA data revealed that the initiation of high P–J mortality (mainly *P. edulis*) across this region began in 2001, with the mortality peaking in 2002–03 (Shaw et al., 2005). Although P–J mortality was estimated to peak around this time across southwestern Colorado, field observations of high P–J mortality did occur in subsequent years (Floyd et al., 2009).

### 2.2. Field data collection

Root collar diameter (RCD, cm) of all live and recently dead P–J plants (reddish or grayish colored needles) were measured from 12 representative plots across a wide spectrum of P–J abundance and tree mortality along an elevation gradient (2000–2300 m) within or nearby Mesa Verde National Park (Fig. 2, lower left inset). These plots were sampled from late spring to early summer (April–July) of 2005, and were geolocated using a high accuracy Trimble Geoexplorer Global Position System (GPS) with post-processing differential correction (Trimble Navigation Limited, Sunnyvale, CA, USA). The size of each plot was 1350 m<sup>2</sup> (45 × 30 m), which was sufficient to cover the local P–J cover variation of a site (Floyd et al., 2004) and matched with the pixel size of moderate spatial resolution satellite images such as Landsat Thematic Mapper (TM). RCD is a measure of the sum of each stem diameter at the ground level (Grier et al., 1992), which is specifically for delineating the structures of multi-stemmed plants such as piñon and juniper trees. Allometric equations were used to estimate AGB (kg) of *P. edulis* and *J. osteosperma* from RCD (cm) (Darling, 1967) where:

$$AGB_{PIED} = 0.024RCD_{PIED}^{2.67} \quad (1)$$

$$AGB_{JUOS} = 0.013RCD_{JUOS}^{2.81} \quad (2)$$

The subscripts PIED and JUOS in Eqs. (1) and (2) are *P. edulis* and *J. osteosperma*, respectively. To our knowledge, these allometric equations are the only available models for the specific P–J plants of the study region. Although no information on model fitness ( $r^2$ ) was reported in Darling (1967), there was an excellent fit based upon visual inspection (approximate estimates of  $r^2 > 0.98$  for both species).

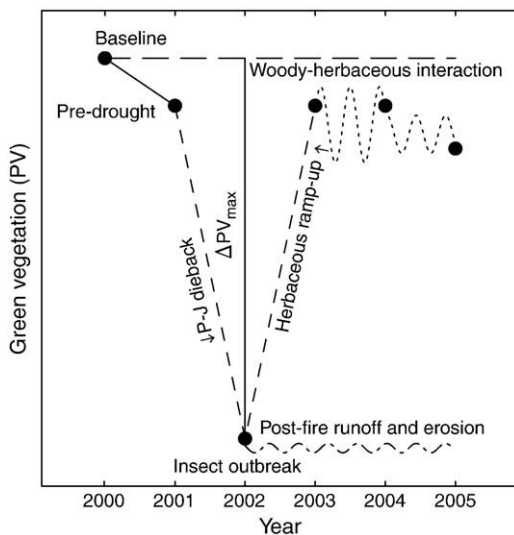
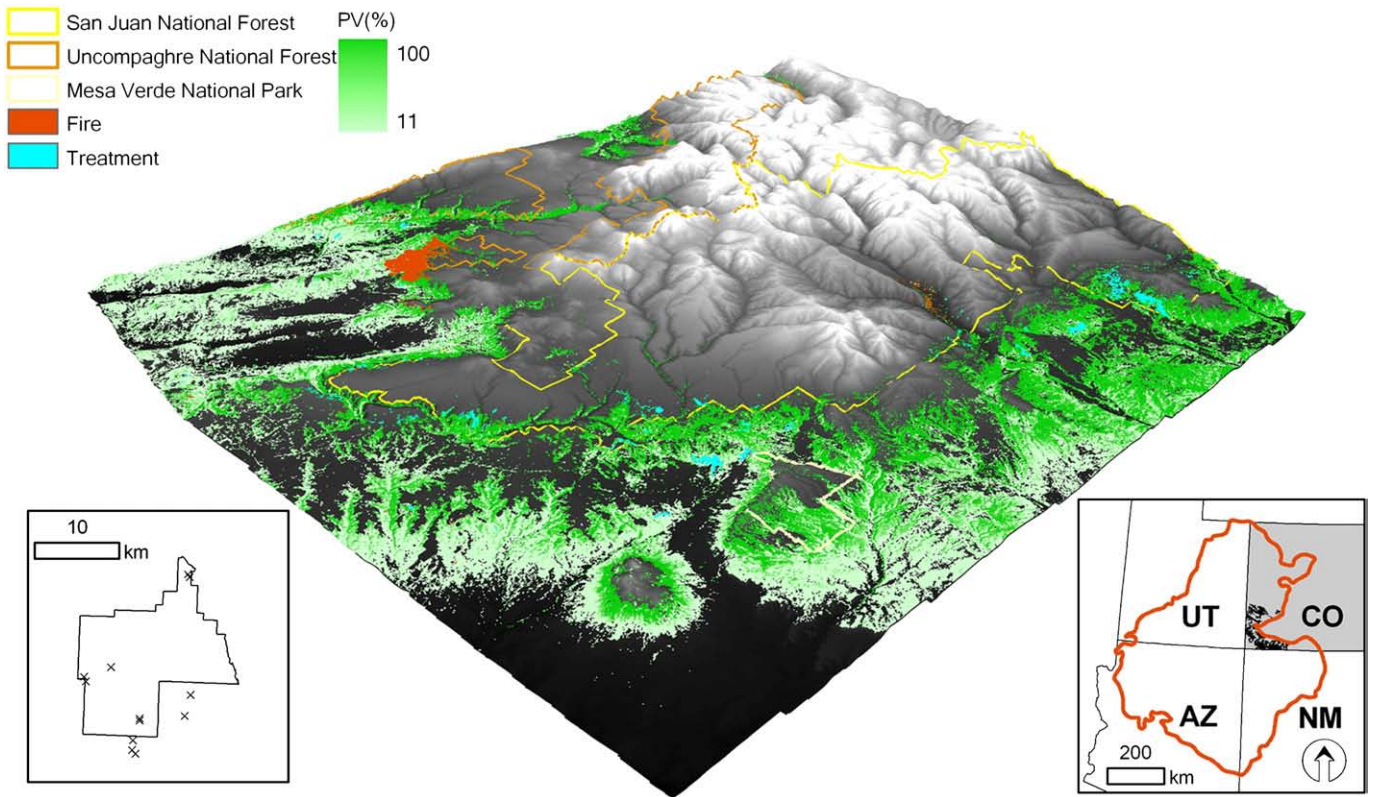


Fig. 1. An illustration of green vegetation (e.g., photosynthetic vegetation cover [PV]) variations and dynamics through the observation period (2000–05) in an area experiencing high tree mortality in the piñon–juniper vegetation.



**Fig. 2.** A three-dimensional view of the study region: piñon–juniper (P–J) vegetation in southwestern Colorado of the Colorado Plateau. The gradient of green-colored layer is the mean photosynthetic vegetation (PV) cover fraction derived from Landsat images acquired in a dry period (Fig. 3); the red and cyan pixels indicate wildfire and management activities (e.g., prescribed fire, commercial timber harvest, thinning), respectively, which occurred during the observation period within and nearby San Juan (yellow outline) or Uncompaghre (orange outlines) National Forests. The background layer is a digital elevation model. The location of study site (dark-colored pixels), boundary of the Colorado Plateau (the red irregular outline) and four southwestern states in the US are displayed in the lower right corner. The light yellow outline is the boundary of Mesa Verde National Park, where dead and live P–J plants were collected. The locations of 12 sampled plots (crosses) are shown in the lower left inset.

Allometry is species-specific and the estimation difference could be substantial. The allometric model consistency of the primary impacted species *P. edulis* was satisfactory (absolute error was 3.8% to the mean) across regions within the Colorado Plateau by comparing

with AGB estimated by Grier et al. (1992) ( $r^2 = 0.95$ ) through a wide range of RCD (from 1 to 80 cm with a 1 cm increment). However, the deviation was very pronounced (absolute error was 71.5%) by comparing *J. osteosperma* with *J. monosperma* ( $r^2 = 0.94$ ; Grier et al.,

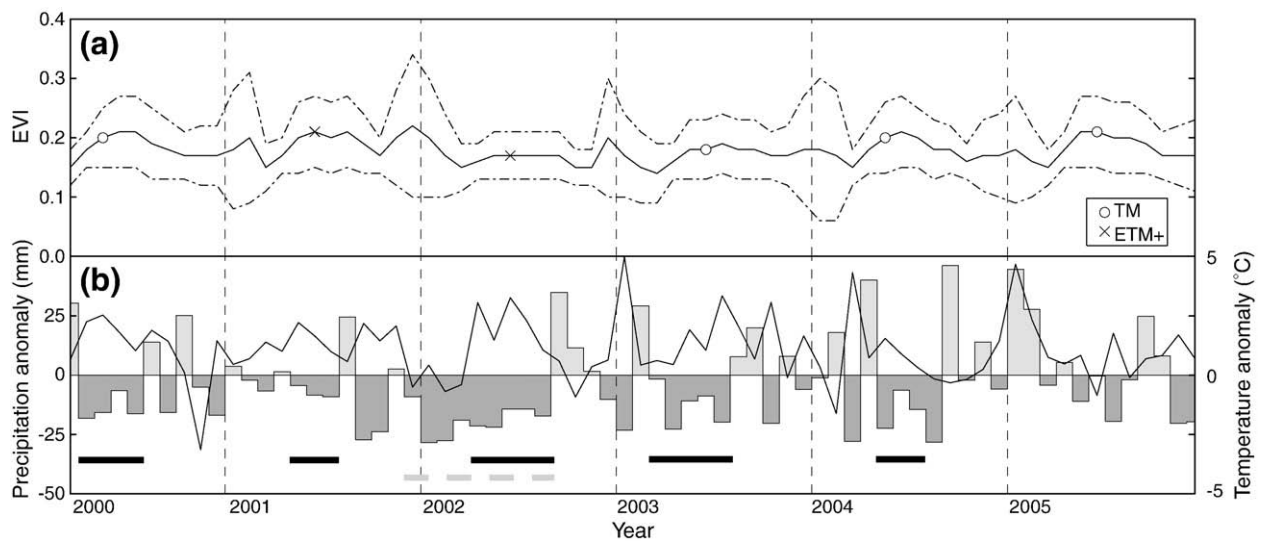


**Fig. 3.** (a) Dynamics of mean MODIS-EVI (the Moderate Resolution Imaging Spectroradiometer-Enhanced Vegetation Index, solid line) ( $\pm$  standard deviation, dash-dotted lines) through the observation period in our study region, which may represent the phenology of the piñon–juniper vegetation. Circles and crosses indicate the months of image acquired by Landsat Thematic Mapper (TM) and Enhanced Thematic Mapper Plus (ETM+), respectively. (b) Anomalies of monthly mean precipitation (left y-axis, above mean: light-colored bars; below mean: dark-colored bars) and temperature (right y-axis, solid line) during the observation period comparing to long-term averages (1895–2006). Black thick lines indicate 3+ consecutive months of dry and hot climate and the gray thick dashed line is the extent of nine consecutive dry months (six of them hotter than the long-term average) during 2001–02.

1992). As a result of our analysis we determined that allometric equations from Darling (1967) were most suitable for this study and cannot be substituted by others.

### 2.3. Analysis of Landsat images

Six Landsat TM and Enhanced Thematic Mapper plus (ETM+) images in WRS-P35R34 with minimum cloud contamination and spanning the 2000 and 2005 time period (Fig. 3a) were acquired from Global Visualization Viewer (<http://glovis.usgs.gov/>). Images were selectively acquired to represent a relative dry period (May and June) of a year before the initiation of summer monsoonal conditions. Landsat TM and ETM+ are multi-spectral sensors that contain six 30 m visible, near infrared and shortwave infrared bands, and one thermal band. These images were from Multi-Resolution Land Characteristics (MRLC) Consortium (<http://www.mrlc.gov/>), and they had been ortho-rectified with high accuracy using a digital elevation model (DEM) prior to the data acquisition.

Time-series PV was derived from these Landsat images using the Carnegie Landsat Analysis System (CLAS). CLAS is an automated Landsat image processing system consisting of three main components: (1) atmospheric correction to estimate surface reflectance from raw data using the 6S model (Vermote et al., 1997); (2) deconvolution of spectral profiles into sub-pixel fractional cover of PV, non-photosynthetic vegetation and bare soils using an automated Monte Carlo unmixing approach (Asner & Heidebrecht, 2002) and (3) cloud/water removal (Asner et al., 2005). A detailed summary of the remote sensing processing procedures can be found in Asner et al. (2006). Since all images were acquired in a dry period and in most cases herbaceous plants were senescent during this time period (see Fig. 3a, the phenology of the P–J vegetation delineated using the time-series Moderate Resolution Imaging Spectroradiometer-Enhanced Vegetation Index [MODIS-EVI], Huete et al., 2002), time-series PV can be directly linked to green P–J cover dynamics through the drought years (Huang et al., 2009). The time-series PV (or P–J cover) should be relatively stable through a short time period unless the occurrence of massive tree mortality due to needle coloration from green to red (Coops et al., 2006). A metric  $\Delta PV_{\max}$  was used in this study indicating the maximum PV reduction comparing to the base year 2000 (Fig. 1):

$$\Delta PV_{\max} = \text{MAX}[|PV_{00} - PV_{01-05}|] \quad (3)$$

where  $PV_{00}$  in Eq. (3) was derived from the 2000 Landsat image and  $PV_{01-05}$  was the PV of 2001–05. Since there was a linear relationship between P–J AGB and Landsat PV (Huang et al., 2009), we expected  $\Delta PV_{\max}$  to be a salient variable for indicating the loss of live P–J AGB. In addition, the occurrence of  $\Delta PV_{\max}$  may imply the year of insect outbreak and high mortality of P–J populations.

### 2.4. Remote sensing estimate of live P–J AGB loss

A regression model was applied to correlate field-estimated live AGB losses (dead P–J plants, dependent variable) and corresponding  $\Delta PV_{\max}$  pixels (independent variable); a regional map of recent live P–J AGB loss could then be generated based upon the correlation. Note that the size of each plot ( $45 \times 30$  m) was slightly greater than a Landsat TM/ETM+ pixel ( $30 \times 30$  m), and plots often intersected two or more pixels. Hence, an area weighting method that assigned different weights for each overlaid pixel based on the area covered was applied to compute representative  $\Delta PV_{\max}$  values for these plots. A leave-one-out, full cross-validation (hereafter “cross-validation”) was used to evaluate the performance of the regression model. Cross-validation is a method to compute prediction error by comparing estimated and true values using only available information. The model omits one sample at a time for all data and predicts the value of that sample using the remaining data (Isaaks & Srivastava, 1989). AGB

losses in areas that had experienced wildfire and management treatments (e.g., chaining, thinning, mowing, prescribed fire and commercial timber harvest) within and nearby the national forests within the observation period (R. Brantlinger, US Forest Service, personal communication) were also computed but were separated in the analysis. These areas were not directly related to P–J dieback, and not only live but majority of dead woody materials may be removed from the ground due to these perturbations. However, in all cases (dieback, wildfire and treatments), the abilities of conducting C sequestration and transporting nutrients and water were lost (van Mantgem et al., 2009) for the damaged plants or portions (e.g., trimmed branches). Note that no disturbance data from state, private, county and tribal lands were available. Nevertheless, a substantial proportion of these lands were located at lower elevation with fewer P–J trees (Fig. 2), and we did not expect significant impacts of these perturbations on regional C stocks.

## 3. Results

### 3.1. Field estimates of live biomass loss

There were 1450 live (825 *P. edulis* and 625 *J. osteosperma*) and 525 dead (439 *P. edulis* and 86 *J. osteosperma*) trees observed in the field. Mean AGB ( $\pm$  standard error) of live *P. edulis* individuals was significantly lower than dead trees (live =  $30.6 \pm 5.3$  kg, dead =  $56.8 \pm 7.3$  kg; Student's *t*-test,  $p = 0.004$ ), but no differences were observed between live and dead *J. osteosperma* (live =  $143.0 \pm 16.7$  kg, dead =  $149.1 \pm 45.1$  kg; Student's *t*-test,  $p = 0.9$ ). The range of P–J density in sampled plots ( $n = 12$ ) was highly variable ( $637$ – $1978$  trees  $\text{ha}^{-1}$ ), and mean density ( $\pm$ sd) was  $1219 \pm 470$  trees  $\text{ha}^{-1}$ . Mean P–J mortality ( $\pm$ sd) was  $28.8 \pm 11.7\%$ , ranging from 14.3 to 49.0%. The majority of the mortality was contributed by *P. edulis*, which comprised 84% of all the dead trees. On average, live P–J AGB declined by  $23.3$  Mg  $\text{ha}^{-1}$ . It was notable that 25% of sampled plots had more than  $32$  Mg  $\text{ha}^{-1}$  of recently dead P–J plants (maximum =  $53.9$  Mg  $\text{ha}^{-1}$ ). Detailed statistics of P–J abundance and mortality in sampled plots are listed in Table 1.

### 3.2. Landsat estimate of biomass loss

There was a significant relationship (linear positive,  $r^2 = 0.64$ ,  $p = 0.002$ ) between field-estimated live P–J AGB losses and  $\Delta PV_{\max}$  (Fig. 4). Mean ( $\pm$ sd) and range of  $\Delta PV_{\max}$ , which was similar to projected P–J cover loss, were  $30.2$  ( $\pm 15.0$ ) % and 11–54%, respectively. Plots with the largest residuals ( $\sim 14$  Mg  $\text{ha}^{-1}$ ) were those with the highest ( $53.9$  Mg  $\text{ha}^{-1}$ ) and lowest ( $3.4$  Mg  $\text{ha}^{-1}$ ) amounts of live AGB losses. The high biomass loss plot had a few large dead trees (e.g., RCD > 40 cm) whereas more than half of the dead trees in the low biomass loss plots were in smaller size classes

**Table 1**

Mean ( $\pm$  standard deviation, sd), minimum and maximum densities, mortality and live aboveground (AGB) losses of *Pinus edulis* (P), *Juniperus osteosperma* (J) and both (P–J) in twelve 1350 m<sup>2</sup> field plots within or nearby Mesa Verde National Park.

		Mean ( $\pm$ sd)	Minimum	Maximum
Density (trees $\text{ha}^{-1}$ )	P	$780 \pm 363$	437	1541
	J	$439 \pm 238$	141	926
	P–J	$1219 \pm 470$	637	1978
Mortality (% density)	P	$39.7 \pm 21.3$	12.5	81.4
	J	$0.1 \pm 0.1$	0.0	0.2
	P–J	$28.8 \pm 11.7$	14.3	49.0
Live AGB loss (Mg $\text{ha}^{-1}$ )	P	$15.4 \pm 13.9$	3.2	53.5
	J	$7.9 \pm 7.8$	0.0	24.1
	P–J	$23.3 \pm 13.3$	3.4	53.9

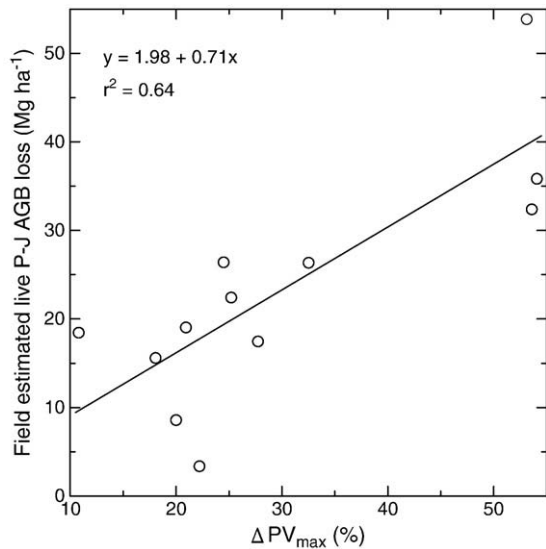


**Fig. 4.** A linear relationship ( $n = 12$ ) between field-estimated live aboveground biomass (AGB) losses of piñon pine and juniper (P-J) and the maximum photosynthetic vegetation reduction ( $\Delta PV_{\max}$ ).

( $RCD \leq 10$  cm). Mean absolute error (the absolute difference between predicted and observed values) ( $\pm$ sd) computed from cross-validation was relatively small ( $7.8 \pm 6.0$  Mg ha $^{-1}$ ) compared to the mean of field observations. This allowed us to map live P-J AGB losses at the regional scale based upon the correlation between the field measure of live P-J AGB losses and  $\Delta PV_{\max}$  (Fig. 5a).

About 78% of  $\Delta PV_{\max}$  occurred during 2001–02 (Fig. 5b). The proportions of the other years were minor (4–10%), and their spatial patterns were rather sparse and difficult to discern in the regional-scale map except for burned areas (Fig. 2). Mesa Verde National Park and nearby Cortez (Montezuma) experienced the largest P-J AGB loss (Fig. 5, upper right inset). Sites with  $>30$  Mg ha $^{-1}$  loss of P-J AGB could be frequently observed within this area. On the other hand, the north part of the region (San Miguel, Montrose and Ouray) experienced little or no P-J dieback (e.g.,  $<10$  Mg ha $^{-1}$  AGB loss). Only a few spots that revealed large P-J AGB losses were caused by wildfire (Fig. 2).

### 3.3. Carbon loss due to dieback and other perturbations

Impacts of wildfire, human activities and drought-related dieback on the structure and C stocks of the P-J vegetation were substantial, as shown in 1-m resolution aerial photos acquired in the 1990s (pre-disturbance) and 2005 (post-disturbance) (Fig. 6). However, the frequency of wildfire and human disturbance was infrequent in the national forests of the study region during the observation period (Fig. 2 and Table 2). Only 1.7% and 0.8% of the P-J vegetation within or near to the national forests experienced wildfire and management treatments, respectively. In contrast,  $\sim 4000$  km $^2$  (97.5% of the study region) indicated losses of live P-J AGB based on the satellite  $\Delta PV_{\max}$  approach (Eq. (3)). Mean drought-related live aboveground C loss ( $\pm$ sd) and mean aboveground C loss ( $\pm$ sd) caused by other perturbations (wildfire and treatment) were  $10.0 (\pm 3.4)$  Mg C ha $^{-1}$  and  $11.4 (\pm 4.0)$  Mg C ha $^{-1}$ , respectively, using a biomass-C conversion coefficient of 0.48 (Schlesinger, 1997). We thus calculated that the total aboveground live C loss due to P-J dieback (4.6 Tg C) was about 39 times the C loss due to wildfire and treatment (0.12 Tg C) in the national forests from 2000 to 2005.

## 4. Discussion

This study used a new remote sensing approach to quantify losses of live *P. edulis* and *J. osteosperma* AGB during a recent multi-year drought; results highlight the importance of regional-scale distur-

bance events in determining changes in North America C storage. In the following sections, we focus on (a) assessing the ramifications of P-J dieback on the regional C stocks; (b) evaluating the feasibility of remote sensing to map P-J AGB loss at the Landsat scale; and (c) discussing the implications for ecological modeling and global C budget assessments.

### 4.1. Impacts of dieback on regional C stocks

The intensity of P-J dieback damage ( $10.0 \pm 3.4$  Mg C ha $^{-1}$ ) on the regional C stocks in terms of loss of plant vitality was close to other destructive perturbations (e.g., wildfire, timber harvest) ( $11.4 \pm 4.0$  Mg C ha $^{-1}$ ) (Table 2). This would equate to 92% and 39% of the total P-J AGB of 90- and 350-year-old P-J young and mature stands, respectively, in a very similar P-J ecosystem (*P. edulis*-*J. monosperma* system) (Grier et al., 1992). The recovery of live C storage in this region could take more than a decade in a young stand and much longer for a mature system since the annual aboveground net primary production of the P-J vegetation was relatively low ( $1.0$ – $1.4$  Mg C ha $^{-1}$  yr $^{-1}$ ) (Grier et al., 1992; Knapp & Smith, 2001) – assuming insect/disease infestation slowed after the recent drought. However, this would not be likely since we found in the field that a substantial proportion of live *P. edulis* was attacked by pinyon ips (*Ips confusus*), a common group of bark beetle, and a majority of these trees will be dead eventually a few years later (Kurz et al., 2008). Therefore, the potential damage may be greater than our estimate.

Our results revealed that drought-related dieback may have become the major source of live C loss in the P-J vegetation of southwestern US, with much greater magnitude than the long existing perturbations of wildfire and human activities. In this study, we found that drought-related live P-J AGB loss was about 39 times greater than P-J AGB loss due to wildfire and human activities during the observation period within/near to national forests. Note that coarse woody debris would remain on the site after dieback and decomposition across these landscapes is generally slow. It will take several decades to release all C to the atmosphere. Hence, impacts of dieback would be more severe in terms of total C fluxes than stocks.

The spatial pattern of live P-J AGB loss in southwest Colorado was heterogeneous (Fig. 5a). Areas of high biomass loss were located in the south mainly encompassed by La Plata, Montezuma and part of Dolores Counties. Our result agreed with FIA's field-based county-level estimate (Shaw et al., 2005) and with a much finer spatial resolution ( $30 \times 30$  m) and greater detail. These would justify the integration of field observations and Landsat derived  $\Delta PV_{\max}$ . The influences of topography to loss of tree C in the P-J vegetation seemed to be varied across the study region by a rough visual comparison to DEM (Fig. 2). Our field observations revealed that large-sized *P. edulis* might be more susceptible to drought and bark beetle attack (mean live *P. edulis* [ $\pm$ sd] =  $30.6 \pm 5.3$  kg; dead *P. edulis* =  $56.8 \pm 7.3$  kg). In the future, by integrating the P-J AGB loss map (Fig. 5a) with large-scale estimates of potential determinants such as climate, topographic conditions and P-J characteristics (e.g., stand-age, size, density, etc.), we might be able to decipher the complexity of the spatial pattern of P-J dieback (Fensham & Holman, 1999; Greenwood & Weisberg, 2008).

P-J woodlands are the most spatially extensive vegetation type in the southwest US (Lowry et al., 2007), and the *P. edulis*-*J. osteosperma* is a dominant community type in the P-J vegetation (West, 1999). Surprisingly, to our knowledge, there are no statistically-validated allometric models available for use at the regional scale. Available models were species-specific, and cannot easily be represented by other species even with similar canopy structures. Without appropriate models, propagated errors may be substantial and difficult to control after interpolating/extrapolating biomass using remote sensing. In the future, a set of statistically-validated allometric models for dominant woody plants of P-J woodlands across regions are

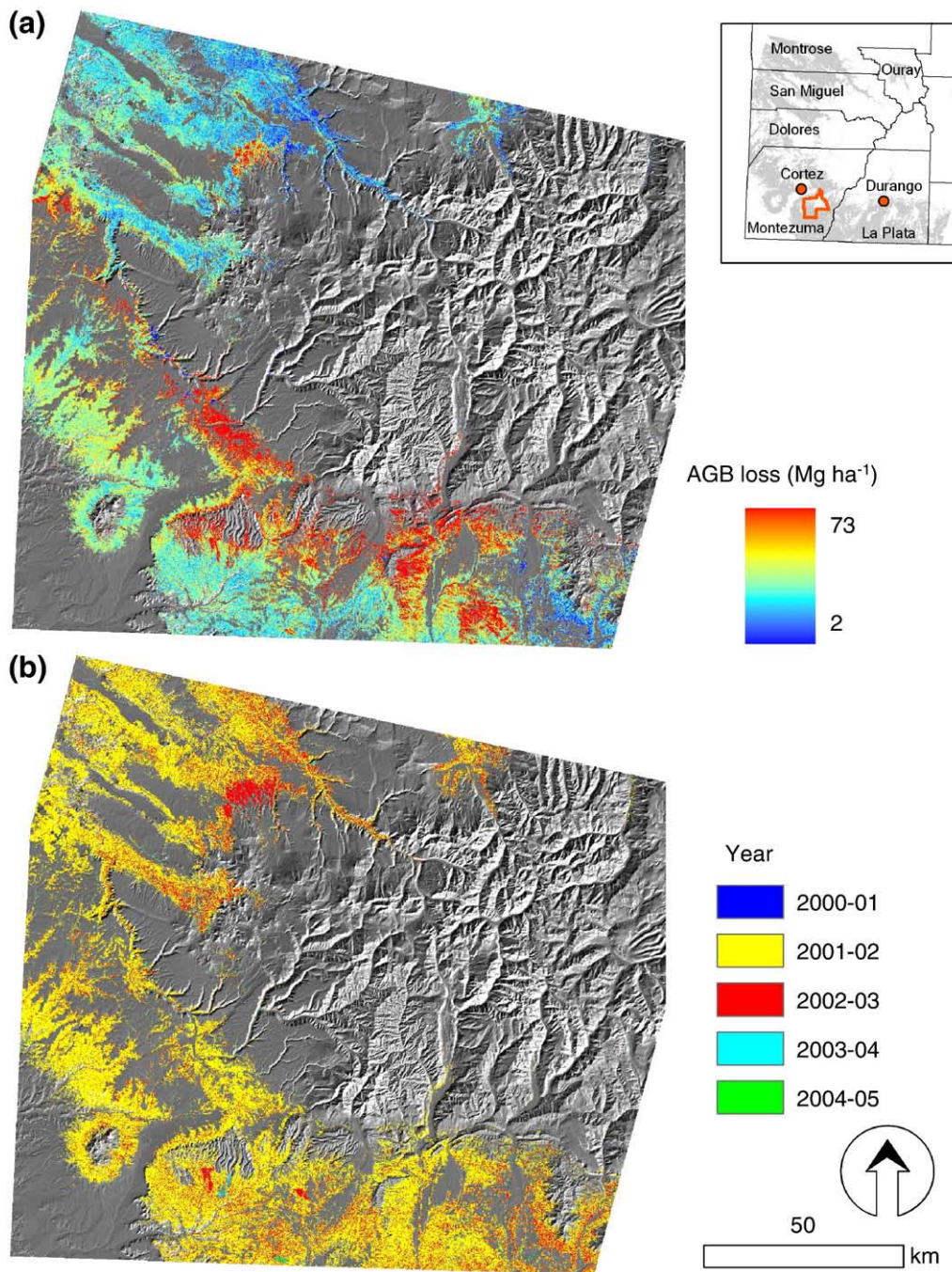


**Fig. 5.** (a) Landsat estimated live piñon-juniper (P-J) aboveground biomass (AGB) losses of the study region. (b) Years of the occurrence of maximum photosynthetic vegetation reduction ( $\Delta PV_{\max}$ , Fig. 1) derived from time-series Landsat images (Fig. 3a). The upper right inset indicates the spatial extent of the P-J vegetation (gray pixels) and political boundaries of the study region (black outlines: counties, the red polygon: Mesa Verde National Park, red dots: Cortez and Durango).

required for the improved assessment of changing C storage in P-J woodlands.

#### 4.2. Remote sensing assessment of P-J dieback

This study demonstrates the feasibility of utilizing time-series dry season Landsat PV ( $\Delta PV_{\max}$ ) to map live P-J AGB loss. A wide range of biomass loss field data collection ( $3.4\text{--}53.9 \text{ Mg ha}^{-1}$ ; Fig. 4) facilitates a fairly robust regional-scale estimate (Fig. 5a). Our approach is straightforward, and it may be applicable to map other impacts of the recent drought on C stocks in P-J ecosystems as well as possibly other

vegetation types provided that the allometric models are available (Grier et al., 1992; Hanson & Weltzin, 2000; Jenkins et al., 2003).

The majority of  $\Delta PV_{\max}$  was detected during 2001–02 (Fig. 5b) that corresponded to the period of high P-J mortality reported by FIA (Shaw et al., 2005). In addition, the  $\Delta PV_{\max}$  approach detected other perturbations. For example, the large wildfire in the northwest region (Burn Canyon Fire) (Fig. 2) occurred in the early July of 2002 (Fig. 5b). This also indicates the high sensitivity of  $\Delta PV_{\max}$  to recognize an abrupt decline of tree cover.

Despite the overall success of our method, there are a few constraints that need to be discussed here. Landsat  $\Delta PV_{\max}$  was most likely to capture the onset of bark beetle infestation occurring in

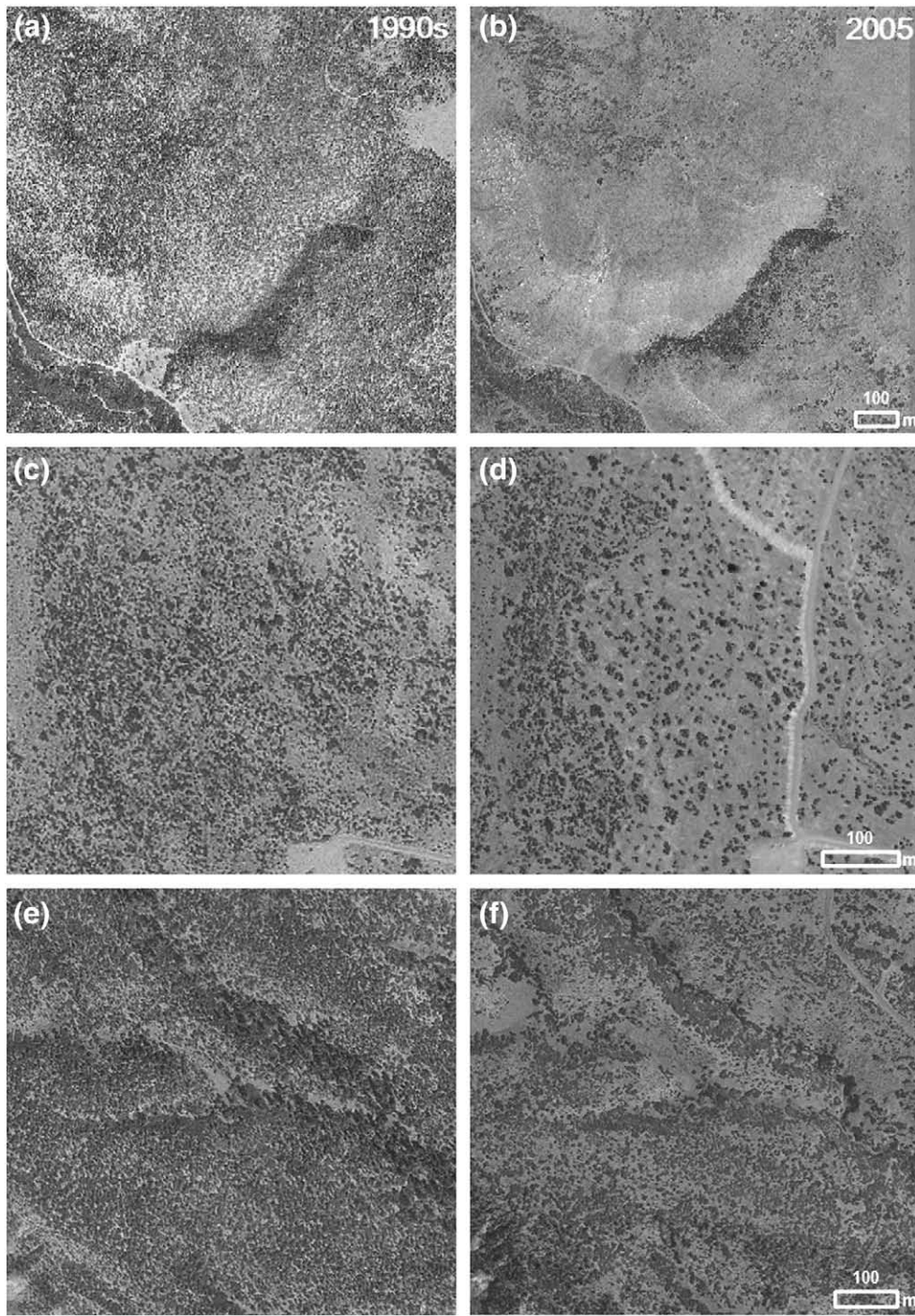


**Fig. 6.** Illustrations of tree loss during the dieback period (2001–05) in the piñon–juniper vegetation of the Colorado Plateau due to wildfire (a: pre-burn; b: post-burn at 38.07° N, 108.44° W), thinning (c: pre-treatment, d: post-treatment at 37.22° N, 107.70° W) and dieback (e: pre-drought; f: post-drought at 37.15° N, 107.95° W) using 1-m resolution aerial photographs obtained in 1990s and 2005. Green tree canopies are shown as dark-colored pixels.

**Table 2**

Mean ( $\pm$  standard deviation, sd) ( $\text{Mg C ha}^{-1}$ ) and total (TgC) aboveground carbon (C) losses during the recent drought due to wildfire, treatment and dieback; and sizes ( $\text{km}^2$ ) (proportion in percentage, %) of these agents within the study region. Note that the spatial data of wildfire and treatment were acquired within and nearby two national forests (San Juan and Uncompaghre).

	Wildfire	Treatment	Dieback
Mean C loss ( $\pm$ sd)	11.4 $\pm$ 4.0	11.4 $\pm$ 3.8	10.0 $\pm$ 3.4
Total C loss	0.1	0.04	4.6
Area (%)	68 (1.7)	34 (0.8)	3970 (97.5)

2002. However, our 2005 field campaign conducted in Mesa Verde National Park included live P–J AGB loss resulting from not only the 2002 massive dieback but the gradual damage of bark beetle attack thereafter (see review by [Wulder et al., 2006](#)). Live P–J AGB loss after the year of  $\Delta\text{PV}_{\text{max}}$  could be difficult to discern since green vegetation may be rapidly offset by the ramp-up of understory shrubs (*P. tridentata*, *Artemisia* species, *A. utahensis* and others) unaffected by the beetle. This might explain a part of the uncertainty in the model. In addition, estimation of woody C is challenging, especially for two-dimensional (2-D) optical remote sensing ([Huang et al., 2009](#)), and some of the limitations were clearly revealed in our  $\Delta\text{PV}_{\text{max}}$  analysis.

Outliers with a few large dead trees producing substantial live AGB loss but relatively small  $\Delta PV_{\max}$ , or those with many small dead trees (low AGB) but relatively large  $\Delta PV_{\max}$  would generate large model residuals due to the nature of the log–log relationship between cover and biomass (Fig. 4). Sensors that can view land surfaces at a 3-D perspective can estimate biomass effectively (e.g., Lefsky et al., 2002; Neeff et al., 2005). However, in our case, the task was even more challenging and required combining both dimensional and spectral information (Treuhaft et al., 2004; Asner et al., 2007) to further improve the assessment of dead AGB.

Another concern is that the minimum detectable live P–J AGB loss was about  $3.4 \text{ Mg ha}^{-1}$  according to the field observations (Fig. 4). Therefore, areas of low biomass loss (Fig. 5a) may not necessarily indicate dieback but the natural fluctuation of green vegetation influenced by dry climate or normal background tree mortality (van Mantgem et al., 2009), and live P–J AGB loss might be slightly overestimated in these lightly impacted areas. However, it would be difficult to decipher these background variations, since they may vary from site to site and could be influenced by various biotic (e.g., density, age class) and abiotic (e.g., topography) factors (e.g., Pennisi, 2009). On the other hand, the accuracy of estimating the larger AGB losses ( $> 53.9 \text{ Mg ha}^{-1}$ ) was difficult to assess since no additional information was available for the validation of our remotely sensed approach. However, the areal coverage of these zones were very small ( $< 0.2\%$ ), and thus should not have a major influence on our overall results. One other technically related issue is mis-geolocation of the field GPS and remote sensing measures that might also generate uncertainty to the model. It can be minimized with the careful selection of a high accuracy GPS instrument and ortho-rectified MRLC Landsat images (e.g., this study).

#### 4.3. Implications on dryland ecosystem modeling and global C assessment

Drylands are often mixed woody–herbaceous systems (Belsky, 1990; McPherson, 1997; Scholes & Archer, 1997). Many have endeavored to understand the interactions and dynamics of these two contrasting life forms (see reviews: House et al., 2003; Sankaran et al., 2004) using conceptual or mathematical models (Sankaran et al., 2005; Scholes & Archer, 1997; Walker & Noy-Meir, 1982 and many others). To our knowledge, drought-induced tree dieback and resulting variations in the herbaceous cover have not been included in dryland ecosystem modeling. This study and several recent reports (Allen, 2007; Breshears et al., 2005; Rich et al., 2008; Shaw et al., 2005) reveal that high tree mortality and subsequent herbaceous dynamics would cause enormous changes in the functioning of ecosystems. This tree demographic factor should be considered for the further refinement of ecosystems models.

Drought-induced tree dieback is a global phenomenon widely reported in different ecosystems from several continents (e.g., Australia: Fensham & Holman, 1999; Europe: Hódar et al., 2003; South America: Suarez et al., 2004; North America: Newman et al., 2006), which may significantly influence large-scale biogeochemical and water cycles, energy flows, and land-surface bioclimatic feedbacks to the atmosphere (Pitman et al., 2004). In the case of the P–J vegetation in North America, ecosystems suffered severe damage due to a complex interaction of drought stress, heat and bark beetle kill (Breshears et al., 2005; Shaw et al., 2005). A warmer and droughty climate might be likely to occur in the foreseeable future for the region (IPCC, 2007), which could further exacerbate tree mortality. This rapid shift in tree demography partially counters the regional trend in P–J expansion (Harris et al., 2003; Strand et al., 2006), and could take many years or even decades for a system to recover under different simulated scenarios (Kurz et al., 2008). Our findings thus contribute to continental- and global-scale C assessments, as well as C-related policy and management (Houghton, 2007).

## 5. Conclusions

Drought-induced tree dieback in drylands may have significant impacts on biogeochemical and water cycles (Breshears et al., 2005). However, incorporation of tree mortality in regional and global C budgets is still rudimentary and largely relying on indirect modeling techniques (Kurz et al., 2008). We developed an empirical approach to investigate the effects of dieback on live C stocks in P–J ecosystems of the Colorado Plateau. Based upon the findings, we concluded that the impact of drought-induced tree dieback on the P–J vegetation was far larger than other disturbances from wildfire and human activities. Severe damage of the P–J vegetation might need several years or even decades to recover. The remote sensing analysis revealed a significant relationship between  $\Delta PV_{\max}$  and field-estimated live P–J AGB losses, which may allow us to estimate regional C dynamics. Our findings could refine ecosystem models for arid and semi-arid environments, and improve C assessments over a vast region, which may further facilitate C management.

## Acknowledgments

We thank the editor Dr. Goetz and four anonymous reviewers for comments that improved the manuscript. This work was supported by the NASA North America Carbon Program (NACP-Asner-01), the Carnegie Institution for Science, and the U.S. National Park Service (CA-1248-00-006).

## References

- Adams, J. B., Smith, M. O., & Gillespie, A. R. (1993). Imaging spectroscopy: Interpretation based on spectral mixture analysis. In C. M. Pieters, & P. A. Englert (Eds.), *Remote geochemical analysis: elemental and mineralogical composition* (pp. 145–166). New York: Cambridge University Press.
- Allen, C. (2007). Interactions across spatial scales among forest dieback, fire, and erosion in northern New Mexico landscapes. *Ecosystems*, 10, 797–808.
- Asner, G. P., Archer, S., Hughes, F. R., Ansley, J. R., & Wessman, C. A. (2003). Net changes in regional woody vegetation cover and carbon storage in Texas drylands, 1937–1999. *Global Change Biology*, 9, 316–335.
- Asner, G. P., Broadbent, E. N., Oliveira, P. J. C., Keller, M., Knapp, D. E., & Silva, J. N. M. (2006). Condition and fate of logged forests in the Brazilian Amazon. *Proceedings of the National Academy of Sciences of the United States of America*, 103, 12947–12950.
- Asner, G. P., & Heidebrecht, K. B. (2002). Spectral unmixing of vegetation, soil and dry carbon cover in arid regions: Comparing multispectral and hyperspectral observations. *International Journal of Remote Sensing*, 23, 3939–3958.
- Asner, G. P., Keller, M., Silva, J. N., Knapp, D. E., Broadbent, E. N., & Oliveira, P. J. C. (2005). Ecology: Selective logging in the Brazilian Amazon. *Science*, 310, 480–482.
- Asner, G. P., Knapp, D. E., Jones, M. O., Kennedy-Bowdoin, T., Martin, R. E., Boardman, J., et al. (2007). Carnegie Airborne Observatory: In-flight fusion of hyperspectral imaging and waveform light detection and ranging (wLiDAR) for three-dimensional studies of ecosystems. *Journal of Applied Remote Sensing*, 1, 013536.
- Belsky, J. A. (1990). Tree/grass ratios in East African savannas: A comparison of existing models. *Journal of Biogeography*, 17, 483–489.
- Bradley, B. A., & Fleishman, E. (2008). Relationships between expanding pinyon–juniper cover and topography in the Central Great Basin. *Journal of Biogeography*, 35, 951–964.
- Breshears, D. D., et al. (2005). Regional vegetation die-off in response to global-change-type drought. *Proceedings of the National Academy of Sciences of the United States of America*, 102, 15144–15148.
- Coops, N. C., Johnson, M., Wulder, M. A., & White, J. C. (2006). Assessment of QuickBird high spatial resolution imagery to detect red attack damage due to mountain pine beetle infestation. *Remote Sensing of Environment*, 103, 67–80.
- Daly, C., Neilson, R. P., & Phillips, D. L. (1994). A statistical-topographic model for mapping climatological precipitation over mountainous terrain. *Journal of Applied Meteorology*, 33, 140–158.
- Darling, M. L. S. (1967). Structure and productivity of a pinyon–juniper woodland in Northern Arizona. PhD thesis. Durham, NC: Duke University 188 pp.
- Fensham, R. J., & Holman, J. E. (1999). Temporal and spatial patterns in drought-related tree dieback in Australian savanna. *Journal of Applied Ecology*, 36, 1035–1050.
- Floyd, M. L., Clifford, M., Cobb, N. S., Hanna, D., Delph, R., Ford, P., et al. (2009). Relationship of stand characteristics to drought-induced mortality in three Southwestern piñon–juniper woodlands. *Ecological Applications*, 19, 1223–1230.
- Floyd, M. L., Hanna, D. D., & Romme, W. H. (2004). Historical and recent fire regimes in piñon–juniper woodlands on Mesa Verde, Colorado, USA. *Forest Ecology and Management*, 198, 269–289.
- Goetz, S. J., Baccini, A., Laporte, N. T., Johns, T., Walker, W., Kellndorfer, J., et al. (2009). Mapping and monitoring carbon stocks with satellite observations: A comparison of methods. *Carbon Balance and Management*, 4, 2.

- Goslee, S. C., Havstad, K. M., Peters, D. P. C., Rango, A., & Schlesinger, W. H. (2003). High-resolution images reveal rate and pattern of shrub encroachment over six decades in New Mexico, U.S.A. *Journal of Arid Environments*, *54*, 755–767.
- Greenwood, D. L., & Weisberg, P. J. (2008). Density-dependent tree mortality in pinyon–juniper woodlands. *Forest Ecology and Management*, *255*, 2129–2137.
- Grier, C. C., Elliott, K. J., & McCullough, D. G. (1992). Biomass distribution and productivity of *Pinus edulis*–*Juniperus monosperma* woodlands of north-central Arizona. *Forest Ecology and Management*, *50*, 331–350.
- Hódar, J. A., Castro, J., & Zamora, R. (2003). Pine processionary caterpillar *Thaumetopoea pityocampa* as a new threat for relict Mediterranean Scots pine forests under climatic warming. *Biological Conservation*, *110*, 123–129.
- Hanson, P. J., & Weltzin, J. F. (2000). Drought disturbance from climate change: Response of United States forests. *Science of the Total Environment*, *262*, 205–220.
- Harris, A. T., Asner, G. P., & Miller, M. E. (2003). Changes in vegetation structure after long-term grazing in pinyon–juniper ecosystems: Integrating imaging spectroscopy and field studies. *Ecosystems*, *6*, 368–383.
- Houghton, R. A. (2007). Balancing the global carbon budget. *Annual Review of Earth and Planetary Sciences*, *35*, 313–347.
- House, J. L., Archer, S., Breshears, D. D., & Scholes, R. J. (2003). Conundrums in mixed woody–herbaceous plant systems. *Journal of Biogeography*, *30*, 1763–1777.
- Huang, C., Asner, G. P., Martin, R., Barger, N., & Neff, J. (2009). Multiscale analysis of tree cover and aboveground carbon stocks in pinyon–juniper woodlands. *Ecological Applications*, *19*, 668–681.
- Huang, C., Marsh, S., McClaran, M., & Archer, S. (2007). Post-fire stand structure in a semi-arid savanna: Cross-scale challenges estimating biomass. *Ecological Applications*, *17*, 1899–1910.
- Huete, A., Didan, K., Miura, T., Rodriguez, E. P., Gao, X., & Ferreira, L. G. (2002). Overview of the radiometric and biophysical performance of the MODIS vegetation indices. *Remote Sensing of Environment*, *83*, 195–213.
- IPCC (2007). Climate change 2007: Impacts, adaptation and vulnerability. *Contribution of working group II to the fourth assessment report of the intergovernmental panel on climate change* (pp. 976). Cambridge, UK: Cambridge University Press.
- Isaaks, E. H., & Srivastava, R. M. (1989). *Applied geostatistics*. New York: Oxford University Press 572 pp.
- Jenkins, J. C., Chojnacky, D. C., Heath, L. S., & Birdsey, R. A. (2003). National-scale biomass estimators for United States tree species. *Forest Science*, *49*, 12–35.
- Knapp, A. K., & Smith, M. D. (2001). Variation among biomes in temporal dynamics of aboveground primary production. *Science*, *291*, 481–484.
- Kurz, W. A., Dymond, C. C., Stinson, G., Rampley, G. J., Neilson, E. T., Carroll, A. L., et al. (2008). Mountain pine beetle and forest carbon feedback to climate change. *Nature*, *452*, 987–990.
- Lefsky, M. A., Cohen, W. B., Parker, G. G., & Harding, D. J. (2002). Lidar remote sensing for ecosystem studies. *BioScience*, *52*, 19–30.
- Lowry, J., et al. (2007). Mapping moderate-scale land-cover over very large geographic areas within a collaborative framework: A case study of the Southwest Regional Gap Analysis Project (SWReGAP). *Remote Sensing of Environment*, *108*, 59–73.
- McPhee, J., Comrie, A. C., & Garfin, G. (2004). *Drought and climate in Arizona: Top ten questions & answers*. Tucson, AZ: University of Arizona Climate Assessment Project for the Southwest (CLIMAS).
- McPherson, G. R. (1997). *Ecology and management of North American savannas*. Tucson, AZ: The University of Arizona Press 208 pp.
- Neeff, T., Dutra, L. V., dos Santos, J. R., Freitas, C. d. C., & Araujo, L. S. (2005). Tropical forest measurement by interferometric height modeling and P-band radar backscatter. *Forest Science*, *51*, 585–594.
- Newman, B. D., et al. (2006). The ecohydrology of arid and semiarid environments: A scientific vision. *Water Resources Research*, *42*, W06302, doi:10.1029/2005WR004141.
- Pennisi, E. (2009). Ecology: Western U.S. forests suffer death by degrees. *Science*, *323*, 447.
- Pitman, A. J., Narisma, G. T., Pielke, R. A., Sr., & Holbrook, N. J. (2004). Impact of land cover change on the climate of southwest Western Australia. *Journal of Geophysical Research-Atmospheres*, *109*, D18109, doi:10.1029/2003JD004347.
- Rich, P. M., Breshears, D. D., & White, A. B. (2008). Phenology of mixed woody–herbaceous ecosystems following extreme events: Net and differential responses. *Ecology*, *89*, 342–352.
- Sankaran, M., et al. (2005). Determinants of woody cover in African savannas. *Nature*, *438*, 846–849.
- Sankaran, M., Ratnam, J., & Hanan, N. P. (2004). Tree–grass coexistence in savannas revisited—insights from an examination of assumptions and mechanisms invoked in existing models. *Ecology Letters*, *7*, 480–490.
- Scanlon, T. M., Albertson, J. D., Caylor, K. K., & Williams, C. A. (2002). Determine land surface fractional cover from NDVI and rainfall time series for a savanna ecosystem. *Remote Sensing of Environment*, *82*, 376–388.
- Schlesinger, W. H. (1997). *Biogeochemistry: an analysis of global change*. San Diego, CA: Academic Press 588 pp.
- Scholes, R. J., & Archer, S. R. (1997). Tree–grass interactions in savannas. *Annual Review of Ecology and Systematics*, *28*, 517–544.
- Shaw, J. D., Steed, B. E., & DeBlander, L. T. (2005). Forest inventory and analysis (FIA) annual inventory answers the question: What is happening to pinyon–juniper woodlands? *Journal of Forestry*, *103*, 280–285.
- Strand, E. K., Smith, A. M. S., Bunting, S. C., Vierling, L. A., Hann, D. B., & Gessler, P. E. (2006). Wavelet estimation of plant spatial patterns in multitemporal aerial photography. *International Journal of Remote Sensing*, *27*, 2049–2054.
- Suarez, M. L., Ghermandi, L., & Kitzberger, T. (2004). Factors predisposing episodic drought-induced tree mortality in *Nothofagus* – site, climatic sensitivity and growth trends. *Journal of Ecology*, *92*, 954–966.
- Treuhaft, R. N., Law, B. E., & Asner, G. P. (2004). Forest attributes from radar interferometric structure and its fusion with optical remote sensing. *BioScience*, *54*, 561–571.
- van Mantgem, P. J., et al. (2009). Widespread increase of tree mortality rates in the western United States. *Science*, *323*, 521–524.
- Vermote, E. F., Tanre, D., Deuze, J. L., Herman, M., & Morcette, J. J. (1997). Second simulation of the satellite signal in the solar spectrum, 6S: An overview. *IEEE Transactions on Geoscience and Remote Sensing*, *35*, 675–686.
- Walker, B. H., & Noy-Meir, I. (1982). Aspects of stability and resilience of savanna ecosystems. In B. J. Huntley, & B. H. Walker (Eds.), *Ecology of tropical savannas* (pp. 556–590). Berlin: Springer-Verlag.
- Weisberg, P. J., Lingua, E., & Pillai, R. B. (2007). Spatial patterns of pinyon–juniper woodland expansion in Central Nevada. *Rangeland Ecology and Management*, *60*, 115–124.
- West, N. E. (1999). Juniper–pinon savannas and woodlands of western North America. In R. C. Anderson, J. S. Fralish, & J. M. Baskin (Eds.), *Savanna, barrens, and rock outcrop plant communities of North America* (pp. 288–308). Cambridge: Cambridge University Press.
- Wulder, M. A., Dymond, C. C., White, J. C., Leckie, D. G., & Carroll, A. L. (2006). Surveying mountain pine beetle damage of forests: A review of remote sensing opportunities. *Forest Ecology and Management*, *221*, 27–41.
- Zheng, D., Rademacher, J., Chen, J., Crow, T., Bressee, M., Le Moine, J., et al. (2004). Estimating aboveground biomass using Landsat 7 ETM+ data across a managed landscape in northern Wisconsin, USA. *Remote Sensing of Environment*, *93*, 402–411.